introns, was deleted and replaced with the neomycin-resistance (*neo*^{r}) gene driven by the mouse phosphoglycerol kinase (PGK1) promoter, in reverse orientation to the *p63* gene. To select against random insertional events, a thymidine kinase (TK) gene under the regulation of MC1 promoter[7] was incorporated at the 5′ end of the targeting vector. The targeting vector contained ~5 kb of homology on each side of the PGK-*neo*^{r} gene. The vector was linearized using a unique *Not*I site and electroporated into the JI ES cell line. G418 and FIAU-resistant ES cell colonies were picked, expanded and screened using probe *a* to hybridize genomic DNA digested with *Bgl*I and *Bam*HI. Probe *a* hybridizes to a DNA fragment of ~13.5 kb corresponding to the wild-type allele, and to a 7.5-kb fragment resulting from the targeted allele. Positive clones were screened with probe *b*, which hybridizes to ~18-kb wild-type fragment and ~22-kb targeted allele upon *Nhe*I digestion Two distinct ES cell lines heterozygous for the disrupted allele were microinjected into blastocysts from B57BL/6 and BALB/c mice, causing germline transmission of the *p63* mutation. Mice heterozygous for the mutant *p63* allele were interbred, and the genotype of progeny determined by Southern blotting as described. Harvard Medical School is an AAALAC accredited institution and the mice were cared for in accordance with institutional guidelines.

Histology and immunohistochemistry. Specimens were fixed in Bouin's fluid, 10% buffered formalin, or 4% paraformaldehyde in PBS, embedded in paraffin, and sectioned at 6 mm. Histological analysis was done on sections stained with haematoxylin and eosin. p63 staining was done with the 4A4 anti-p63 monoclonal antibody[1]; K-5, loricrin, involucrin, and filaggrin staining was with rabbit polyclonal antibodies[24,27] (provided by P. Dotto and H. Green).

***In situ* hybridization.** Non-radioactive whole-mount *in situ* hybridization of mouse embryos was done essentially as described[18]. Probes used were: ΔNp63γ (ref. 1), Wnt7a (ref. 19), FGF-8 (ref. 12), and Lmx1b (ref. 17).

Received 21 January; accepted 17 March 1999.

1. Yang, A. *et al.* p63, a p53 homolog at 3q27-29, encodes multiple products with transactivating, death-inducing, and dominant-negative activities. *Mol. Cell* **2,** 305–316 (1998).
2. Augustin, M., Bamberger, C., Paul, D. & Schmale, H. Cloning and chromosomal mapping of the human p53-related KET gene to chromosome 3q27 and its murine homolog Ket to mouse chromosome 16. *Mamm. Genome* **11,** 899–902 (1998).
3. Osada, M. *et al.* Cloning and functional analysis of human p51, which structurally and functionally resembles p53. *Nature Med.* **4,** 839–843 (1998).
4. Trink, B. *et al.* A new human p53 homologue. *Nature Med.* **4,** 747–748 (1998).
5. Ko, L. J. & Prives, C. p53: puzzle and paradigm. *Genes Dev.* **10,** 1054–1072 (1996).
6. Kaghad, M. *et al.* Monoallelically expressed gene related to p53 at 1p36, a region frequently deleted in neuroblastoma and other human cancers. *Cell* **90,** 809–819 (1997).
7. Mansour, S. L., Thomas, K. R. & Capecchi, M. R. Disruption of the proto-oncogene *int-2* in mouse embryo-derived stem cells: a general strategy for targeting mutations to non-selectable genes. *Nature* **336,** 348–352 (1988).
8. Tickle, C. Vertebrate limb development. *Curr. Opin. Genet. Dev.* **5,** 478–484 (1995).
9. Johnson, R. L. & Tabin, C. J. Molecular models for vertebrate limb development. *Cell* **90,** 979–990 (1997).
10. Kelley, R. O. & Fallon, J. F. Ultrastructural analysis of the apical ectodermal ridge during vertebrate limb morphogenesis. I. The human forelimb with special reference to gap junctions. *Dev. Biol.* **51,** 241–256 (1976).
11. Francis-West, P., Ladher, R., Barlow, A. & Graveson, A. Signalling interactions during facial development. *Mech. Dev.* **75,** 3–28 (1998).
12. Crossley, P. H., Minowada, G., MacArthur, C. A. & Martin, G. R. Roles for FGF-8 in the induction, initiation, and maintenance of chick limb development. *Cell* **84,** 127–136 (1996).
13. Vogel, A., Rodriguez, C. & Izpisua-Belamonte, J. C. Involvement of FGF-8 in initiation, outgrowth, and patterning of the vertebrate limb. *Development* **122,** 1737–1750 (1996).
14. Loomis, C. A., Kimmel, R. A., Tong, C. X., Michaud, J. & Joyner, A. L. Analysis of the genetic pathway leading to formation of ectopic apical ectodermal ridges in mouse Engrailed-1 mutant limbs. *Development* **125,** 1137–1148 (1998).
15. Roberts, B., Lyons, G., Simandl, B. K., Kuroiwa, A. & Buckingham, M. The apical ectodermal ridge regulates Hox-7 and Hox-8 gene expression in developing chick limb buds. *Genes Dev.* **5,** 2362–2374 (1991).
16. Wang, Y. & Sassoon, D. Ectoderm–mesenchyme and mesenchyme–mesenchyme interactions regulate Msx-1 expression and cellular differentiation in the murine limb bud. *Dev. Biol.* **168,** 374–382 (1995).
17. Chen, H. *et al.* Limb and kidney defects in Lmx1b mutant mice suggest an involvement of LMX1B in human nail patella syndrome. *Nature Genet.* **19,** 51–55 (1998).
18. Riddle, R. D. *et al.* Induction of the LIM homeobox gene Lmx1 by WNT7a establishes dorsoventral pattern in the vertebrate limb. *Cell* **83,** 631–640 (1995).
19. Parr, B. A. & McMahon, A. P. Dorsalizing signal Wnt-7a required for normal polarity of D–V and A–P axes of mouse limb. *Nature* **374,** 350–353 (1995).
20. Pellegrini, G. *et al.* Location and clonal analysis of stem cells and their differentiated progeny in the human ocular surface. *J. Cell Biol.* (in the press).
21. Byrne, C., Tainsky, M. & Fuchs, E. Programming gene expression in developing epidermis. *Development* **120,** 2369–2383 (1994).
22. Rheinwald, J. G. & Green, H. Serial cultivation of strains of human epidermal keratinocytes: the formation of keratinizing colonies from single cells. *Cell* **6,** 331–344 (1975).
23. Barrandon, Y. & Green, H. Three clonal types of keratinocytes with different capacities for multiplication. *Proc. Natl Acad. Sci. USA* **84,** 2302–2306 (1987).
24. Barrandon, Y. The epidermal stem cell: an overview. *Dev. Biol.* **4,** 209–215 (1993).
25. Watt, F. M. Epidermal stem cells: markers, patterning and the control of stem cell fate. *Phil. Trans. R. Soc. Lond. B* **358,** 553–560 (1991).
26. Greer, J. & Roop, D. Loricrin, a major keratinocyte envelope protein, is expressed late in development. *J. Invest. Term.* **96,** 553–560 (1991).
27. Calautti, E., Missero, C., Stein, P. L., Ezzell, R. M. & Dotto, G. P. Fyn tyrosine kinase is involved in keratinocyte differentiation control. *Genes Dev.* **9,** 2279–2291 (1995).
28. Jan, Y. N. & Jan, L. Y. Asymmetric cell division. *Nature* **392,** 775–778 (1998).
29. Donehower, L. A. *et al.* Mice deficient for p53 are developmentally normal but susceptible to spontaneous tumours. *Nature* **356,** 215–221 (1992).
30. Jacks, T. *et al.* Tumor spectrum analysis in p53 mutant mice. *Curr. Biol.* **4,** 1–7 (1994).

Acknowledgements. We thank H. Green, M. Kirschner, P. Dotto, B. Olsen, N. Fukai, T. Rapoport, B. Quade, J. Glickman, P. Ferrara and T. Bestor for their support and for discussion; H. Green, G. Martin, A. McMahon, R. Johnson, A. Joyner and P. Dotto for reagents; L. Du for blastocyst injections; H. Liu for the 129 mouse genomic library; and J. Williams for histology preparations. This work was supported by grants from the NIH to R.B., C.T., A.S. and F.M.

Correspondence and requests for materials should be addressed to F.McK. (e-mail: frank_mckeon@hms.harvard.edu).

MCP-1 and IL-8 trigger firm adhesion of monocytes to vascular endothelium under flow conditions

Robert E. Gerszten*†, Eduardo A. Garcia-Zepeda†‡, Yaw-Chyn Lim†§, Masayuki Yoshida‖, Han A. Ding§, Michael A. Gimbrone Jr†§, Andrew D. Luster†‡, Francis W. Luscinskas†§ & Anthony Rosenzweig*†

** The Cardiovascular Research Center and Cardiology Division, Massachusetts General Hospital, Boston, Massachusetts 02114, USA*
† Harvard Medical School, Boston, Massachusetts 02114, USA
‡ Infectious Disease Unit, Massachusetts General Hospital, Boston, Massachusetts 02114, USA
§ Vascular Research Division, Department of Pathology, Brigham and Women's Hospital, Boston, Massachusetts 02115, USA
‖ Molecular Genetics, Medical Research Institute, Tokyo Medical and Dental University, Tokyo, Japan

Monocytes contribute to the development of atherosclerotic lesions in mouse models[1–3]. The chemoattractant proteins (chemokines), monocyte chemoattractant protein-1 (MCP-1) and interleukin-8 (IL-8), are found in human atheroma[4,5], and mice lacking receptors for these chemokines are less susceptible to atherosclerosis and have fewer monocytes in vascular lesions[6,7]. Although MCP-1 has a powerful effect on monocytes, IL-8 is thought to act predominantly on neutrophils and it is unclear how it could recruit monocytes[6,8]. Here we investigate the ability of chemokines to control the interaction of monocytes under flow conditions with vascular endothelium that has been transduced to express specific leukocyte-adherence receptors. We find that MCP-1 and IL-8 can each rapidly cause rolling monocytes to adhere firmly onto monolayers expressing E-selectin, whereas related chemokines do not. These effects do not correlate with either the induction of a calcium transient or chemotaxis. We conclude that chemokines are important modulators of monocyte–endothelial interactions under flow conditions. Moreover, our finding that IL-8 is a powerful trigger for firm adhesion of monocytes to vascular endothelium reveals an unexpected role for this chemokine in monocyte recruitment.

To investigate the mechanisms of monocyte adhesion, we used recombinant adenoviruses containing specific endothelial adhesion molecules to transduce human umbilical vein endothelial cells (HUVEC), a well characterized model of vascular endothelium. The initial tethering of monocytes to vascular endothelium can be mediated by vascular-cell adhesion molecule-1 (VCAM-1), but we found that VCAM-1 alone was unable to support firm monocyte adhesion under flow as well as cytokine-activated endothelium could[9], indicating that other signals expressed by activated endothelial cells were enhancing monocyte recruitment[9]. At relatively higher shear ($\geq$1.5 dynes cm^{-2}), the initial rate of monocyte attachment to

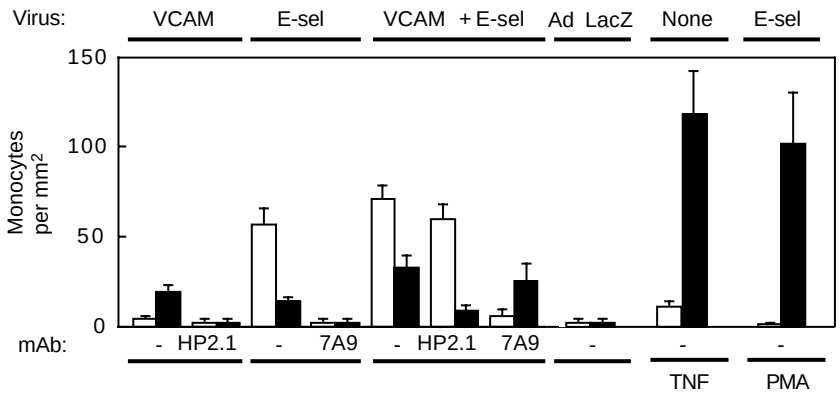

Figure 1 Monocyte attachment to adenovirally transduced or cytokine-activated HUVEC. Endothelial monolayers were transduced with AdVCAM-1, AdE-sel, or both, or with AdRSVβgal(LacZ), or were stimulated with TNF for 4 h immediately before the experiment. 48 h after infection, the interaction of monocytes with these monolayers was studied at 2.0 dynes cm^{-2}. The phenotype of sustained monocyte–endothelial interactions was characterized as either 'rolling' (white bars) or 'firm adhesion' (black bars)[19]. AdVCAM-1 supported predominantly monocyte firm adhesion, whereas AdE-sel supported predominantly monocyte rolling. Compared to VCAM-1 alone, co-expression of E-selectin with VCAM-1 greatly increased monocyte rolling ($n = 7, P < 0.001$) with only a modest increase in firm adhesion ($n = 7, P < 0.02$). In contrast, TNF-activated HUVEC supported much more monocyte firm adhesion ($n = 6, P < 0.001$) and less rolling ($n = 6, P < 0.001$) than did doubly transduced HUVEC. Monoclonal antibodies (HP2.1) against the VCAM-1 counterligand (α4-integrin) effectively blocked monocyte adhesion to AdVCAM-transduced HUVEC ($n = 3, P < 0.001$). HP2.1 also blocked monocyte firm adhesion to doubly transduced HUVEC ($n = 3, P < 0.01$), resulting in predominantly monocyte rolling. A monoclonal antibody (mAb) (7A9) directed at E-selectin blocked all monocyte interactions with AdE-sel-transduced HUVEC ($n = 3, P < 0.001$) and restored a pattern similar to that seen with the expression of VCAM-1 alone. Activation of monocytes with PMA (100 ng ml^{-1}) increased monocyte firm adhesion to E-selectin-transduced monolayers to levels comparable to those seen in TNF-activated HUVEC ($n = 3, P$ = NS). Data shown (± s.e.m.) are pooled from nine experiments, with each condition tested the indicated number of times.

HUVEC activated by tumour-necrosis factor (TNF) significantly exceeded the attachment to VCAM-1-transduced HUVEC. Co-expression of E-selectin with VCAM-1 significantly increased primary monocyte–endothelial interactions (data not shown), but these interactions manifested mainly as monocyte rolling, rather than as firm adhesion (Fig. 1). Thus, vascular endothelium expressing E-selectin and VCAM-1 at levels comparable to those in cytokine-activated HUVEC supports more monocyte rolling and less adhesion than do TNF-activated HUVEC. In contrast, activation of monocytes with phorbol myristate acetate (PMA; 100 ng ml^{-2} for 5 min at 37 °C) enhances firm adhesion even to monolayers transduced with E-selectin alone, to a similar extent to cytokine-activated endothelium (Fig. 1). These results suggest that leukocyte activation is important for monocyte recruitment, so we have investigated the ability of chemokines, as pathophysiologically relevant leukocyte activators expressed by cytokine-treated HUVEC, to mediate the conversion of monocyte rolling to firm adhesion.

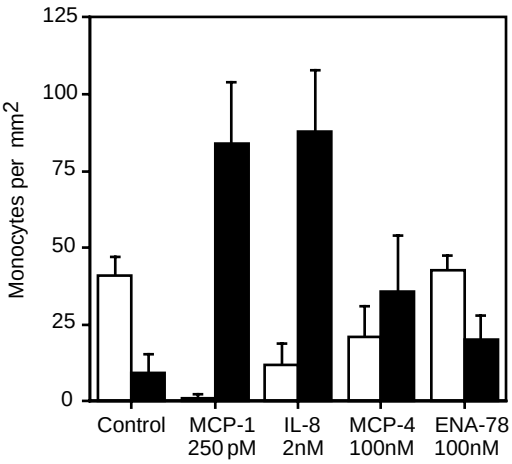

Figure 2 MCP-1 and IL-8 induce arrest of monocytes. Endothelial monolayers were transduced with AdE-sel and cultured for 48 h. Monocytes were perfused at a shear stress of 2.0 dynes cm^{-2}. The indicated chemokine was added to the monocyte reservoir (room temperature) and monocyte rolling (white bars) and firm adhesion (black bars) were quantified for each coverslip 1 min before and 1 min after addition of the chemokine. MCP-1 (250 pM; $n = 3$) and IL-8 (2 nM; $n = 7$) converted virtually all monocyte rolling to firm adhesion within 1 min ($P < 0.001$ for firm adhesion compared with before chemokine addition). In contrast, MCP-4 induced at most a modest increase in monocyte firm adhesion at doses up to 100 nM ($n = 5, P < 0.01$ compared with IL-8 or MCP-1). ENA-78 did not significantly affect monocyte rolling ($n = 5, P$ = NS). Data (±s.e.m.) are pooled from seven experiments, with each condition tested the indicated number of times.

Chemokines were added to monocytes being perfused over E-selectin-transduced monolayers, as a model of selectin-mediated monocyte rolling. Monocyte rolling and firm adhesion were quantified for each HUVEC monolayer one minute before and one minute after addition of the chemokine. Recombinant MCP-1 (a CC chemokine) at concentrations ≥250 pM effectively transformed virtually all monocyte rolling to firm adhesion (Fig. 2), whereas MCP-4, a CC chemokine that induces monocyte chemotaxis and Ca^{2+} transients at doses as low as 2.5 nM (ref. 10), only moderately increased monocyte firm adhesion, even at 100 nM. Surprisingly, IL-8 (a CXC chemokine) at concentrations ≥2 nM induced monocyte firm adhesion comparable to that seen after MCP-1 treatment (Fig. 2), whereas epithelial-derived neutrophil-activating protein (ENA)-78 (Fig. 2) and other CXC chemokines (IP-10 and PF-4; data not shown) had little or no effect on E-selectin-dependent monocyte rolling. IL-8-induced monocyte arrest occurred with recombinant chemokine from two different commercial sources and was prevented by monoclonal antibody against IL-8 (data not shown). Several factors indicate that the effect on adhesion was not due to the *de novo* recruitment of other leukocytes such as neutrophils, which might contaminate the monocyte preparations. First, the purity of the starting population was confirmed by both flow cytometry and histochemical staining. Second, histochemically stained coverslips after IL-8 or MCP-1 treatment were reviewed by clinical haematologists blinded to the treatment protocol: in each case, adherent leukocytes were a homogeneous population with the

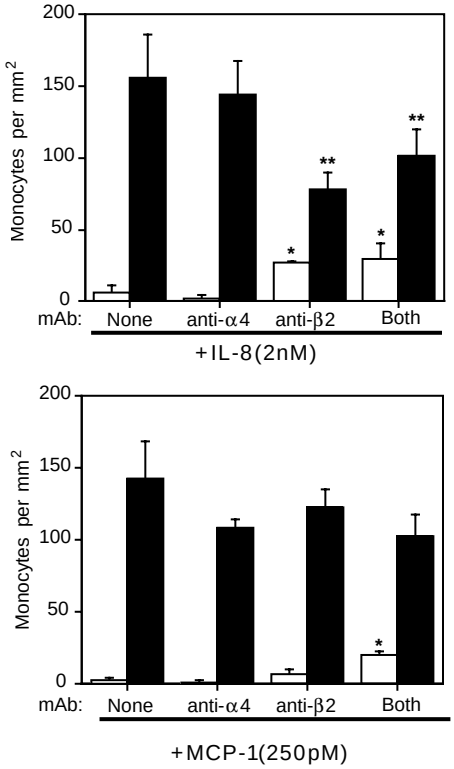

Figure 3 MCP-1 and IL-8 augment arrest by using different integrins. HUVEC monolayers were infected with AdE-sel and cultured for 48 h. Monocytes were incubated with the indicated mAb for 10 min at 4 °C immediately before the experiment. IL-8-induced monocyte arrest (black bars) was significantly blocked by an mAb (TS1/18) to β2 integrin ($P < 0.01$ compared with no mAb), with restoration of the rolling phenotype (white bars, $P < 0.001$), whereas an mAb to α4 integrin (HP2/1) had no effect on IL-8-induced firm adhesion (top). In contrast, mAbs to α4 or β2 integrin alone did not affect MCP-1-induced monocyte adhesion. In combination, these mAbs could restore some monocyte rolling after MCP-1 treatment ($P < 0.05$), although no significant decrease in overall adhesion was noted (bottom). Binding antibody to class I MHC (W6/32) did not affect adhesion either (data not shown). Representative data are one of four experiments. Single asterisk indicates a significant increase in monocyte rolling. Double asterisks indicate a significant decrease in monocyte firm adhesion.

morphology of monocytes (data not shown). Finally, we monitored the effect of the chemokine on rolling leukocytes by videomicroscopy. The firm leukocyte adhesion seen after IL-8 or MCP-1 treatment reflected the arrest of virtually all rolling leukocytes, rather than recruitment of a different population from the flow stream. Thus, both IL-8 and MCP-1 arrested monocytes interacting with E-selectin-expressing vascular endothelium.

To investigate the adhesive mechanisms contributing to monocyte arrest in this system, we used function-blocking monoclonal antibodies to the α4 and β2 leukocyte integrins. A number of counterligands for these integrins are constitutively expressed by vascular endothelium, including intercellular adhesion molecule-1 and fibronectin[11]. IL-8-induced monocyte arrest was significantly

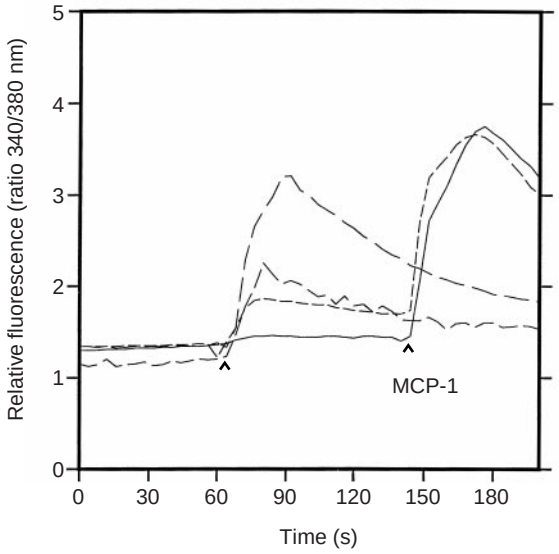

Figure 4 Chemokine-induced calcium flux in human monocytes. Fura-2-loaded monocytes were exposed to MCP-1 (2 nM; long-dash line), MCP-4 (2.5 nM; medium-dash line), IL-8 (10 nM; short-dash line), or ENA-78 (100 nM; solid line) at the time indicated (left caret). The data are presented as the relative ratio of fluorescence at 340 and 380 nm. MCP-1 induced a strong response; MCP-4 and IL-8 induced smaller calcium transients. ENA-78 did not elicit calcium flux at doses of up to 100 nM. A subsequent strong response to MCP-1 was recorded in the ENA-78 and IL-8-treated samples (right caret).

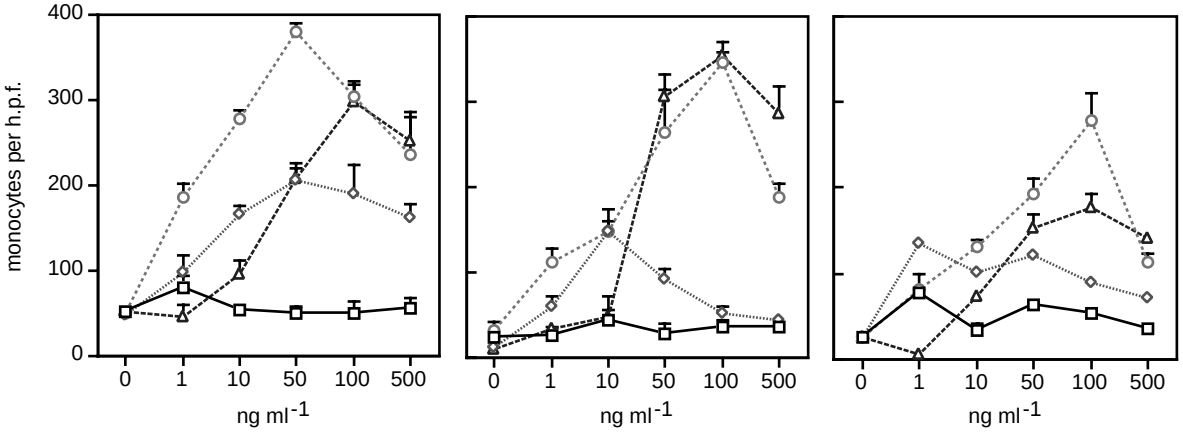

Figure 5 Chemotaxis of elutriated monocytes. Purified monocytes in a modified Boyden chamber were exposed to MCP-1 (circles), MCP-4 (triangles), IL-8 (diamonds) or ENA-78 (squares) at the indicated concentrations. After 90 min, the cells that migrated through the membrane were counted in three high-power fields (h.p.f.) from each duplicate well. Data (±s.d.) are shown from three independent chemotaxis experiments using monocytes elutriated from different donors, done in parallel with flow experiments. In each experiment, IL-8 induced significantly more monocyte chemotaxis than did ENA-78 ($P < 0.0001$ at 10 and 50 ng ml^{-1}).

blocked by a monoclonal antibody to β2 integrin (TS1/18), with restoration of the rolling phenotype (Fig. 3, top). A monoclonal antibody to α4 integrin (HP2/1) had no effect on IL-8-induced firm adhesion. In contrast, neither of these antibodies alone affected MCP-1-induced monocyte adhesion, but in combination they restored some monocyte rolling despite MCP-1 treatment (Fig. 3, bottom). These results indicate that, although IL-8 and MCP-1 both trigger the firm adhesion of monocytes, the contribution of specific integrin adhesion receptors to the induced adhesion differs for these two agonists, perhaps because they use different signalling mechanisms. There is early activation of β1 integrins (α4β1 and α5β1) in both monocytes[12] and T lymphocytes[13] after MCP-1 treatment, which may have important implications for transendothelial chemotaxis. In contrast, we found that function-blocking monoclonal antibodies to α4 had little effect under flow conditions, which probably reflects the absence of the principal endothelial β1 counterligand, VCAM-1, as well as differences in the monocyte–endothelial interaction.

Given that the CXC chemokine IL-8, but not the CC chemokine

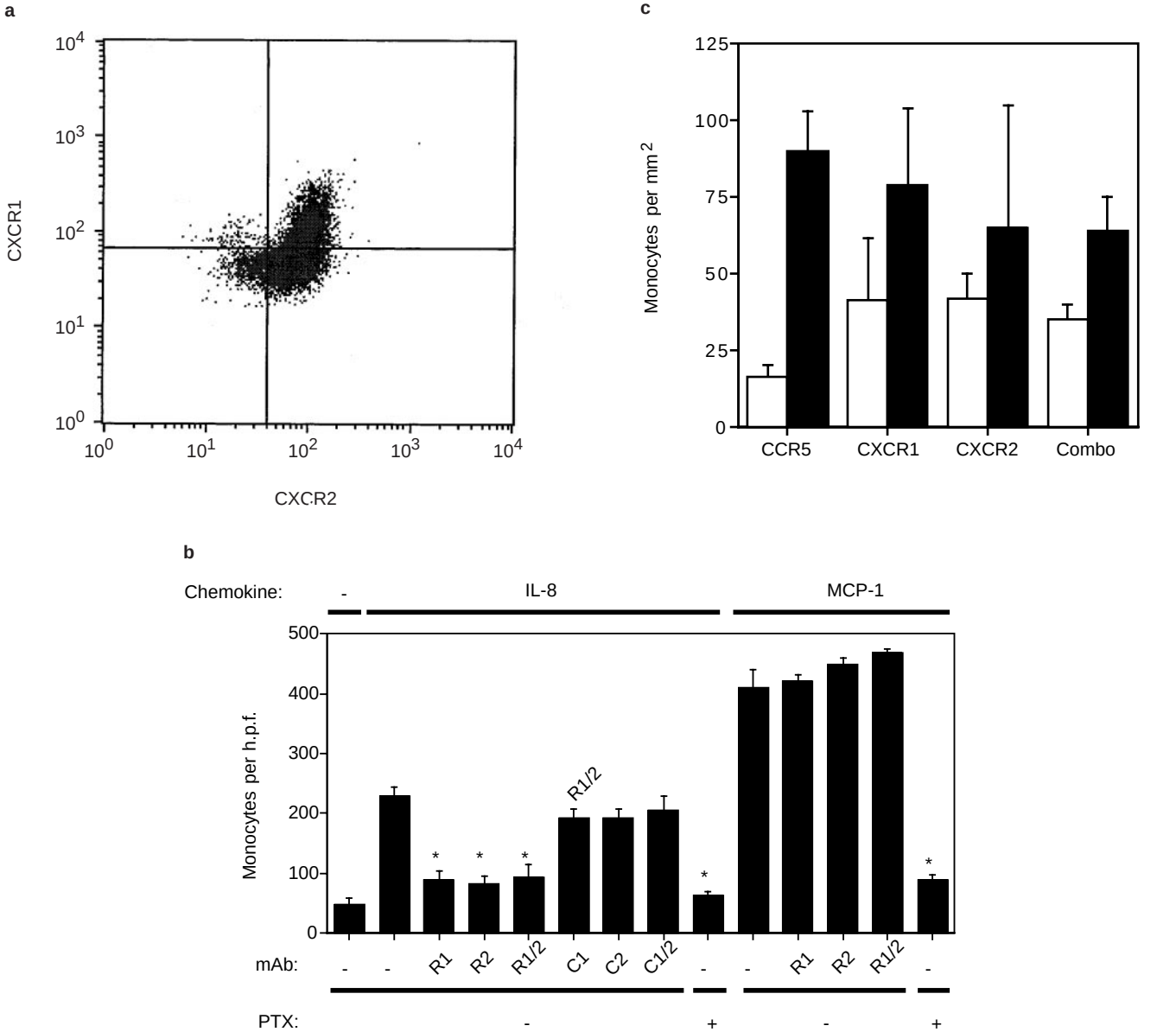

Figure 6 Monocytes express functional IL-8 receptors. **a**, Surface expression of CXCR1 and CXCR2 on elutriated monocytes. Monocytes were subjected to flow cytometry with fluorescently labelled mAb to CD14 (APC), CXCR1 (FITC) and CXCR2 (PE) (see Methods). Surface expression of CXCR1 and CXCR2 on CD14-positive cells is shown from one of four independent experiments. **b**, mAb to CXCR1 and CXCR2 inhibit IL-8 induced monocyte chemotaxis. Purified monocytes were incubated with the indicated mAb and then exposed to MCP-1 or IL-8 (both at 50 ng ml^{-1}) in a modified Boyden chamber. After 90 min, the cells that migrated through the membrane were counted in three high-power fields from each duplicate well. Representative data are from one of three independent experiments. In each experiment, treatment with mAb to CXCR1 (R1), CXCR2 (R2) or both (R1/2) significantly reduced monocyte chemotaxis to IL-8 but not to MCP-1 ($P < 0.001$ compared with IL-8 alone or treatment with isotype-matched control mAb, C1 for IgG_1 and C2 for IgG_{2A}). Pretreatment of monocytes with pertussis toxin (PTX: 250 ng ml^{-1} for 2 h at 37 °C) blocked monocyte chemotaxis to both IL-8 and MCP-1 ($P < 0.001$ compared with chemokine alone). **c**, mAbs to CXCR1 and CXCR2 restored monocyte rolling after IL-8 treatment. HUVEC monolayers were infected with AdE-sel as above and cultured for 48 h. Monocytes were incubated with the indicated mAb for 10 min at 4 °C immediately before the experiment. Monocyte rolling (white bars) and firm adhesion (black bars) were quantified 1 min after IL-8 (2 nM) addition. Representative data are from one of three experiments. Simultaneous treatment with mAbs raised against CXCR1 and CXCR2 (combo) significantly preserved the rolling phenotype as compared with control mAb ($P < 0.05$ for the experiment shown and for pooled data from all three experiments).

MCP-4, could trigger firm adhesion of monocytes at nanomolar concentrations under laminar flow, we tested whether these chemokines could induce calcium flux in elutriated monocytes. MCP-1 (2 nM) and MCP-4 (2.5 nM) both stimulate a large and rapid rise in intracellular calcium in monocytes (Fig. 4)[10]; IL-8 produces a small dose-dependent calcium flux in monocytes (Fig. 4), consistent with previous reports[8]. Therefore, the ability of chemokines to trigger adhesion of monocytes under flow to E-selectin-transduced endothelium does not correlate with their ability to stimulate a rise in intracellular calcium in monocytes. Moreover, the concentrations of MCP-1 and IL-8 that stimulate calcium transients in monocytes were consistently higher than those required to trigger firm adhesion of monocytes. Our assay evidently reveals an extremely sensitive biological effect.

We tested whether IL-8 could function as a monocyte agonist in other physiologically relevant models by chemotaxis assays. Although donor variability was evident, IL-8 consistently induced significant monocyte chemotaxis with a smaller maximal effect than that seen with MCP-1 or -4 (Fig. 5). In all cases, histochemical staining confirmed that the transmigrated cells were monocytes (data not shown). Moreover, checkerboard analysis performed in parallel in two experiments demonstrated that IL-8 induced monocyte chemotaxis rather than simple chemokinesis (data not shown). Although IL-8-induced monocyte chemotaxis has not been detected before[14,15], we used elutriated monocytes rather than cells isolated by adherence to substrate, which may alter the functional phenotype of monocytes[16]. As MCP-4 is more potent than IL-8 in inducing both a calcium transient and monocyte chemotaxis (Figs 4 and 5) but is less effective at converting monocyte rolling to firm adhesion (Fig. 2), these effects are presumably mediated by divergent intracellular signalling pathways.

IL-8 binds to two known receptors in humans, CXCR1 and CXCR2 (ref. 17), although only a homologue of CXCR2 has been found in mice[6]. One or both receptors were present on the surface of most of the elutriated monocytes used here (Fig. 6a). In three out of four donors, CXCR2 expression was more prevalent than CXCR1 expression, consistent with previous reports[16], although the relative prevalence varied widely among monocyte donors. CXCR1 was expressed on 23–90% of the elutriated monocytes, and CXCR2 was expressed on 22–93%. Pretreatment of monocytes with monoclonal antibodies raised against either of these receptors significantly reduced monocyte chemotaxis to IL-8 but not to MCP-1 (Fig. 6b). Simultaneous treatment with both antibodies partially restored monocyte rolling after IL-8 treatment (Fig. 6c). In combination, these antibodies also inhibited IL-8-induced calcium transients (data not shown). As further confirmation of receptor-mediated signalling, pertussis toxin also blocked IL-8-induced chemotaxis (Fig. 6b); however, the same experiment could not be done for adhesion under flow because pertussis toxin activated the monocytes, as shown by loss of surface L-selectin and increased β1 integrin activation epitopes on flow cytometry (data not shown), and it altered the baseline phenotype of monocyte–endothelial interaction. Nevertheless, the cumulative data indicate that the IL-8 receptors on monocytes[16] are functional and account for the observed phenomena. ENA-78, which binds CXCR2, did not induce significant monocyte chemotaxis (Fig. 5) or firm adhesion (Fig. 2). These results are consistent with a model in which both receptors are necessary but neither alone is sufficient for the IL-8 effects, perhaps because the receptors interact cooperatively (as reported for other members of this receptor family[18]) or because their downstream signalling pathways may converge.

Our results indicate that specific chemokines are essential for monocyte recruitment not only as chemoattractants, but also by translating initial monocyte tethering into firm adhesion through activation of leukocyte integrin. The *in vitro* model presented here provides a sensitive system for investigating this control by chemokines and reveals an important biological effect that is not predicted by results of simpler *in vitro* assays, such as measurement of calcium transients or chemotaxis. The unexpected finding that the CXC chemokine IL-8 can trigger monocyte firm adhesion to vascular endothelium indicates a potential role for this chemokine in monocyte recruitment and reinforces the biological complexity of the chemokine family. Identification of the vascular signals responsible for monocyte recruitment could provide insight into the cellular and molecular mechanisms of atherogenesis and suggest new targets for therapeutic intervention. □

Methods

Materials. RPMI 1640, DMEM and DPBS with or without Ca^{2+} and Mg^{2+} were purchased from BioWhittaker; HSA was from Baxter Healthcare; FBS was from Hyclone; recombinant hTNF-α was from Biogen. Recombinant chemokines were generously provided by PeproTech or purchased from R&D Systems. Pertussis toxin was purchased from Calbiochem.

Cell culture. HEK 293 cells were obtained from the American Type Culture Collection and cultured in DMEM supplemented with 10% FBS as described[9]. HUVEC were isolated and cultured as described[19] in M199 with 20% FBS, endothelial-cell growth factor (25 μg ml^{-1}; Biomedical Technologies), porcine intestinal heparin (50 μg ml^{-1}; Sigma), and antibiotics; after infection with adenoviral vectors, HUVEC were cultured in 10% FBS. For stimulation of HUVEC, recombinant hTNF-α (200 U ml^{-1}) was added as indicated. For experimental use in the flow-plate apparatus, HUVEC (passage 1–2) were plated at confluence on 25-mm fibronectin-coated glass coverslips as described[19]; infection of HUVEC has been described[9]. On the day of the flow adhesion assay, a fluorescence immunoassay was done on HUVEC infected in parallel to determine transgene expression and to rule out nonspecific activation of the endothelial monolayer[9].

Recombinant adenoviruses. Three recombinant type-5 adenoviruses (Ad) were used in these studies: AdRSVβ-gal, AdVCAM-1, and AdE-sel. All three viruses have a similar backbone, containing *E1/E3* deletions. AdRSVβ-gal was a gift from D. A. Dichek (Gladstone Institute for Cardiovascular Diseases). The construction of AdVCAM-1 and AdE-sel has been described[20,21]. Large-scale production of advenovirus and determination of viral titre was done as described[9]. Only one viral stock of each construct was used. Stock titre was 10^{10} PFU ml^{-1} for both vectors, with a particle per PFU ratio of ~10^2.

Monoclonal antibodies. The following mAb were used as purified IgG and have been described: 7A9 (ref. 22) and H4/18 (to human E-selectin[23]), Hu5/3 (to human ICAM-1; ref. 24), E1/6 (which recognizes both human and rabbit VCAM-1; ref. 25), HP2.1 (to α_4-integrin; Immunotech), 5A12 (to CXCR1; Pharmingen), 6C6 (to CXCR2; Pharmingen), 2D7 (to CCR5; Leukosite), IgG_1 and IgG_{2A} nonbinding control mAb (Pharmingen).

Flow cytometry. Monocytes were washed once with RPMI/5% FCS and incubated with the indicated fluorescently tagged primary antibodies for 30–60 min on ice, washed twice with RPMI/5% FCS, and fixed with 1% formaldehyde. An isotype-matched, fluorescently labelled nonbinding antibody was included as a control. Fluorescence was then analysed using a Becton–Dickinson FACS set to detect fluorescence, forward scatter and size.

Leukocyte isolation. Human monocytes were purified from single-donor human platelet pheresis residues by Ficoll–Hypaque density-gradient centrifugation at 15 °C (LSM; Organon Teknika), followed by counterflow centrifugation elutriation as described[26]. Monocyte suspensions were >91% pure, with 6–8% lymphocyte, 2% granulocyte and essentially no platelet contamination, as determined by light scatter and cell-surface antigen analysis[26].

Adhesion assays under flow. The parallel-plate flow chamber and assay protocols have been described[19,27]. For endothelial-blocking experiments, HUVEC monolayers were incubated immediately before the assay with culture medium containing the indicated mAb or culture medium alone for 30 min at 37 °C. For monocyte blocking, leukocytes were incubated with the indicated mAb for 10 min at 4 °C and diluted with perfusion medium to 10^6 cells per ml. Where indicated, chemokines were added to the monocyte reservoir (room temperature). Monocyte rolling and firm adhesion were quantified for each coverslip[19] 1 min before and 1 min after addition of chemokine. The cells were perfused at an estimated shear stress of 2.0 dynes cm^{-2} (flow rate of 0.78 ml min^{-1}). The entire period of perfusion was recorded on tape using a video recorder equipped with a time–date generator with a millisecond clock.

Calcium flux in monocytes. Elutriated human monocytes (10^7 ml^{-1}) were loaded with 1.0 μM Fura-2 AM (Molecular Probes) in the dark for 15 min at 37 °C in DPBS containing 0.1% HSA, and intracellular calcium was measured as described[28]. The data are presented as the relative ratio of fluorescence at 340 and 380 nm.

Chemotaxis assays. Chemotaxis assays were carried out in a 48-well microchemotaxis chamber (NeuroProbe) at 37 °C for 90 min[29] on elutriated monocytes in HBSS buffer (MediaTech) supplemented with 0.05% low endotoxin BSA (Sigma) at 5×10^6 cells ml^{-1}. Monocytes that migrated across the filter and adhered to the bottom side were stained with Diff-Quick (Baxter Scientific). The cells per three 400× fields in duplicate wells were counted and the data expressed as the mean ± standard deviation.

Statistical analysis. Data are expressed as the mean ± standard deviation or standard error of the mean, as indicated. Statistical comparison of means was performed by two-tailed unpaired Student's *t*-test. The null hypothesis was considered to be rejected at $P < 0.05$.

Received 4 February; accepted 2 March 1999.

1. Smith, J. D. *et al.* Decreased atherosclerosis in mice deficient in both macrophage colony-stimulating factor (op) and apolipoprotein E. *Proc. Natl Acad. Sci. USA* **92,** 8264–8268 (1995).
2. Suzuki, H. *et al.* A role for macrophage scavenger receptors in atherosclerosis and susceptibility to infection. *Nature* **386,** 292–296 (1997).
3. Fazio, S. *et al.* Increased atherosclerosis in mice reconstituted with apolipoprotein E null macrophages. *Proc. Natl Acad. Sci. USA* **94,** 4647–4652 (1997).
4. Nelken, N. A., Coughlin, S. R., Gordon, D. & Wilcox, J. N. Monocyte chemoattractant protein-1 in human atheromatous plaques. *J. Clin. Invest.* **88,** 1121–1127 (1991).
5. Koch, A. E. *et al.* Enhanced production of the chemotactic cytokines interleukin-8 and monocyte chemoattractant protein-1 in human abdominal aortic aneurysms. *Am. J. Pathol.* **142,** 1423–1431 (1993).
6. Boisvert, W. A., Santiago, R., Curtiss, L. K. & Terkeltaub, R. A. A leukocyte homologue of the IL-8 receptor CXCR-2 mediates the accumulation of macrophages in atherosclerotic lesions of LDL receptor-deficient mice. *J. Clin. Invest.* **101,** 353–363 (1998).
7. Boring, L., Goslin, J., Cleary, M. & Charo, I. Decreased lesion formation in CCR2–/– mice reveals a role for chemokines in the initiation of atherosclerosis. *Nature* **394,** 894–897 (1998).
8. Baggiolini, M., Dewald, B. & Moser, B. Interleukin-8 and related chemokines—CXC and CC chemokines. *Adv. Immunol.* **55,** 97–179 (1994).
9. Gerszten, R. E. *et al.* Adhesion of monocytes to vascular cell adhesion molecule-1-transduced human endothelial cells: implications for atherogenesis. *Circ. Res.* **82,** 871–878 (1998).
10. Berkhout, T. A. *et al.* Cloning, *in vitro* expression, and functional characterization of a novel human CC chemokine of the monocyte chemoattractant protein (MCP) family that binds and signals through the CC chemokine receptor 2B. *J. Biol. Chem.* **272,** 16404–16413 (1997).
11. Springer, T. A. Traffic signals for lymphocyte recirculation and leukocyte emigration: the multistep paradigm. *Cell* **76,** 301–314 (1994).
12. Weber, C., Alon, R., Moser, B. & Springer, T. A. Sequential regulation of alpha 4 beta 1 and alpha 5 beta 1 integrin avidity by CC chemokines in monocytes: implications for transendothelial chemotaxis. *J. Cell Biol.* **134,** 1063–1073 (1996).
13. Woldemar-Carr, M., Alon, R. & Springer, T. A. The C-C chemokine MCP-1 differentially modulates the avidity of β1 and β2 integrins on T lymphocytes. *Immunity* **4,** 179–187 (1996).
14. Yoshimura, T. *et al.* Purification of a human monocyte-derived neutrophil chemotactic factor that has peptide sequence similarity to other host defense cytokines. *Proc. Natl Acad. Sci. USA* **84,** 9233–9237 (1987).
15. Schroder, J. M., Mrowietz, U., Morita, E. & Christophers, E. Purification and partial biochemical characterization of a human monocyte-derived, neutrophil-activating peptide that lacks interleukin 1 activity. *J. Immunol.* **139,** 3474–3483 (1987).
16. Chuntharapai, A., Lee, J., Hebert, C. A. & Kim, K. J. Monoclonal antibodies detect different distribution patterns of IL-8 receptor A and IL-8 receptor B on human peripheral blood leukocytes. J. Immunol. **153,** 5682–5688 (1994).
17. Premack, B. A. & Schall, T. J. Chemokine receptors: gateways to inflammation and infection. *Nat. Med.* **2,** 1174–1178 (1996).
18. Jones, K. A. *et al.* GABA(B) receptors function as a heteromeric assembly of the subunits GABA(B)R1 and GABA(B)R2. *Nature* **396,** 674–679 (1998).
19. Luscinskas, F. W. *et al.* Monocyte rolling, arrest and spreading on IL-4-activated vascular endothelium under flow is mediated via sequential action of L-selectin, beta 1-integrins, and beta 2-integrins. *J. Cell Biol.* **125,** 1417–1427 (1994).
20. Gerszten, R. *et al.* Adhesion of memory lymphocytes to VCAM-1-transduced human vascular endothelial cells under simulated physiological flow conditions *in vitro*. *Circ. Res.* **79,** 1205–1215 (1996).
21. Yoshida, M., Szente, B. E., Kiely, J.-M., Rosenzweig, A. & Gimbrone, M. A. Regulation of E-selectin phosphorylation during leukocyte adhesion: a novel outside-in signaling role for E-selectin. *J. Immunol.* **161,** 933–941 (1997).
22. Graber, N. *et al.* T cells bind to cytokine-activated endothelial cells via a novel, inducible sialoglycoprotein and endothelial leukocyte adhesion molecule-1. *J. Immunol.* **145,** 819–830 (1990).
23. Bevilacqua, M. P., Prober, J. S., Mendrick, D. L., Cotran, R. S. & Gimbrone, M. A. Identification of an inducible endothelial-leukocyte adhesion molecule. *Proc. Natl Acad. Sci. USA* **84,** 9238–9242 (1987).
24. Luscinskas, F. W. *et al.* Cytokine-activated human endothelial monolayers support enhanced neutrophil transmigration via a mechanism involving both endothelial-leukocyte adhesion molecule-1 and intercellular adhesion molecule-1. *J. Immunol.* **146,** 1617–1625 (1991).
25. Taichman, D. B. *et al.* Tumor cell surface alpha 4 beta 1 integrin mediates adhesion to vascular endothelium: demonstration of an interaction with the N-terminal domains of INCAM-110/VCAM-1. *Cell Regul.* **2,** 347–355 (1991).
26. Luscinskas, F. W. *et al.* L- and P-selectins, but not CD49d (VLA4) integrins, mediate monocyte initial attachment to TNF-activated vascular endothelium *in vitro*. *J. Immunol.* **156,** 326–335 (1996).
27. Shen, J., Luscinskas, F. W., Connolly, A., Dewey, C. F. J. & Gimbrone, M. A. Fluid shear stress modulates cytosolic free calcium in vascular endothelial cells. *Am. J. Physiol.* **262,** C384–390 (1992).
28. Wheeler, M. E., Luscinskas, F. W., Bevilacqua, M. P. & Gimbrone, M. A. Cultured human endothelial cells stimulated with cytokines or endotoxin produce an inhibitor of leukocyte adhesion. *J. Clin. Invest.* **82,** 1211–1218 (1988).
29. Falk, W., Goodwin, R. H. Jr & Leonard, E. J. A 48-well micro chemotaxis assembly for rapid and accurate measurement of leukocyte migration. *J. Immunol. Meth.* **33,** 239–247 (1980).

Acknowledgements. We thank K. Case and W. Atkinson for preparation of human endothelial cell cultures; L. Li and Q. Qui for technical assistance; P. Kaltofen for help with manuscript preparation; M. Cybulsky for rabbit VCAM-1 cDNA and antibody Rb1/9; D. Dichek for help in construction of AdVCAM-1 and for AdRSV β-gal; Leukosite for antibody 2D7; I. Charo for reviewing the manuscript; Z. N. Demirjian and other members of the MGH Clinical Hematology Laboratory for their review of leukocyte morphology. We acknowledge support from the NIH (R.E.G., A.R., M.A.G., F.W.L., A.D.L.). A.R. is an Established Investigator of the American Heart Association.

Correspondence and requests for materials should be addressed to A.R. (e-mail: rosenzweig@helix.mgh.harvard.edu).

Tyro-3 family receptors are essential regulators of mammalian spermatogenesis

Qingxian Lu*†, Martin Gore*†‡, Qing Zhang§, Todd Camenisch‖, Sharon Boast§, Franca Casagranda¶, Cary Lai#, Michael K. Skinner☆, Rüdiger Klein¶, Glenn K. Matsushima‖, H. Shelton Earp, Stephen P. Goff§ & Greg Lemke***

** Molecular Neurobiology Laboratory, Salk Institute for Biological Studies, La Jolla, California 92037, USA*
§ Howard Hughes Medical Institute and Department of Biochemsitry & Molecular Biophysics, Columbia University College of Physicians and Surgeons, New York, New York 10032, USA
*‖ Neuroscience Center and Department of Microbiology & Immunology, and ** Lineberger Comprehensive Cancer Center, University of North Carolina, Chapel Hil, North Carolina 27599, USA*
¶ Developmental Biology Programme, European Molecular Biology Laboratory, 69117 Heidelberg, Germany
 # Department of Neuropharmacology, Scripps Research Institute, La Jolla, California 92037, USA
☆ Center for Reproductive Biology, Department of Genetics and Cell Biology, Washington State University, Pullman, Washington 99164, USA
† These authors contributed equally to this work.

We have generated and analysed null mutations in the mouse genes encoding three structurally related receptors with tyrosine kinase activity: Tyro 3, Axl, and Mer[1–4]. Mice lacking any single receptor, or any combination of two receptors, are viable and fertile, but male animals that lack all three receptors produce no mature sperm, owing to the progressive death of differentiating germ cells. This degenerative phenotype appears to result from a failure of the tropic support that is normally provided by Sertoli cells of the seminiferous tubules, whose function depends on testosterone and additional factors produced by Leydig cells[5–7]. Tyro 3, Axl and Mer are all normally expressed by Sertoli cells during postnatal development, whereas their ligands, Gas6 and protein S, are produced by Leydig cells before sexual maturity, and by both Leydig and Sertoli cells thereafter. Here we show that the concerted activation of Tyro 3, Axl and Mer in Sertoli cells is critical to the role that these cells play as nurturers of developing germ cells. Additional observations indicate that these receptors may also be essential for the tropic maintenance of diverse cell types in the mature nervous, immune and reproductive systems.

The receptor protein-tyrosine kinases (PTKs) of the mammalian Tyro 3 family[8] include Tyro 3 (also named Rse, Sky, Brt, Tif, Dtk, Etk-2)[2,9,10], Axl (also named Ark, Ufo, Tyro 7)[3,11,12] and Mer (also named Eyk, Nyk, Tyro 12)[4,13]). These three receptors are widely expressed in adult tissues, but their function is unknown. They share a distinctive structure, with extracellular regions composed of two immunoglobulin-related domains linked to two fibronectin type-III repeats, and cytoplasmic regions that contain an intrinsic PTK domain. Tyro 3, Axl and Mer are present in variable amounts in

‡ Present address: Arena Pharmaceuticals, San Diego, California 92121, USA (M.G.).